Visualization of altered neurovascular coupling in chronic stroke patients using multimodal functional MRI

Jakob U Blicher[1,2], Charlotte J Stagg[3], Jacinta O'Shea[3], Leif Østergaard[2],
Bradley J MacIntosh[4], Heidi Johansen-Berg[3], Peter Jezzard[3] and Manus J Donahue[3,5,6]

[1]Research Unit, Hammel Neurocentre, Aarhus University Hospital, Hammel, Denmark; [2]CFIN, Aarhus University Hospital, Hammel, Denmark; [3]FMRIB Centre, Nuffield Department of Clinical Neurosciences, University of Oxford, Oxford, UK; [4]Department of Medical Biophysics, University of Toronto, Toronto, Canada; [5]Departments of Radiology, Psychiatry, Physics and Neurology, Vanderbilt University, Nashville, Tennessee, USA; [6]Vanderbilt Memory and Alzheimer's Center, Vanderbilt University, Nashville, Tennessee, USA

Evaluation of cortical reorganization in chronic stroke patients requires methods to accurately localize regions of neuronal activity. Blood oxygenation level-dependent (BOLD) functional magnetic resonance imaging (fMRI) is frequently employed; however, BOLD contrast depends on specific coupling relationships between the cerebral metabolic rate of oxygen ($CMRO_2$), cerebral blood flow (CBF), and volume (CBV), which may not exist following stroke. The aim of this study was to understand whether CBF-weighted (CBFw) and CBV-weighted (CBVw) fMRI could be used in sequence with BOLD to characterize neurovascular coupling mechanisms poststroke. Chronic stroke patients ($n = 11$) with motor impairment and age-matched controls ($n = 11$) performed four sets of unilateral motor tasks (60 seconds/30 seconds off/on) during CBFw, CBVw, and BOLD fMRI acquisition. While control participants elicited mean BOLD, CBFw, and CBVw responses in motor cortex ($P < 0.01$), patients showed only mean changes in CBF ($P < 0.01$) and CBV ($P < 0.01$), but absent mean BOLD responses ($P = 0.20$). BOLD intersubject variability was consistent with differing coupling indices between CBF, CBV, and $CMRO_2$. Thus, CBFw and/or CBVw fMRI may provide crucial information not apparent from BOLD in these patients. A table is provided outlining distinct vascular and metabolic uncoupling possibilities that elicit different BOLD responses, and the strengths and limitations of the multimodal protocol are summarized.

Introduction

Improved management of cerebrovascular disease has reduced stroke-related mortality over the past several decades (Langhorne *et al*, 1993). However, many stroke survivors remain impaired with <25% able to perform prestroke equivalent levels of physical activity 6 months poststroke (Duncan *et al*, 2000). The development and evaluation of novel rehabilitation strategies may be accelerated by improving our understanding of positive cortical reorganization, or cerebral plasticity.

Physiological neuroimaging studies have greatly increased our understanding of cerebral plasticity and learning in the healthy brain. Nevertheless, important challenges must be overcome to translate this knowledge into new treatments (Cheeran *et al*, 2009). Specifically, in stroke recovery research, novel training regimens and/or pharmacological facilitation require a means to evaluate how interventions modulate plasticity related to functional recovery. Neuronal and hemodynamic reorganization occur over different anatomical scales during motor recovery: local rearrangement within primary motor cortex, increased activity in ipsilesional nonprimary sensorimotor areas, and increased activity in the uninjured hemisphere (Johansen-Berg, 2007). To date, neuroimaging techniques such as magnetic resonance imaging (MRI) and positron emission tomography have not consistently demonstrated a clear relationship between radiological findings,

rehabilitation, and long-term prognosis (Buma *et al*, 2010).

Functional MRI (fMRI), most frequently utilizing blood oxygenation level-dependent (*BOLD*) contrast, represents the most popular avenue for evaluating recovery, as it can be performed in patients without the use of exogenous contrast agents or ionizing radiation (Ogawa *et al*, 1990). The *BOLD* fMRI response depends on the net change in capillary and venous blood oxygenation that result from disproportionate changes in cerebral blood flow (*CBF*), cerebral blood volume (*CBV*), and the cerebral metabolic rate of oxygen consumption (*CMRO₂*). Under conditions of healthy brain function, a positive *BOLD* signal arises due to a larger increase in *CBF* relative to $CMRO_2$, leading to a reduction in relative concentration of paramagnetic deoxy-hemoglobin in capillaries and veins. Neurovascular coupling, however, is known to be altered in stroke, hypertension, and atherosclerosis, possibly disturbing the coupling of *CBF* and *CBV* to $CMRO_2$, and lowering cerebrovascular reserve capacity (Derdeyn *et al*, 2002; Girouard and Iadecola, 2006; Roc *et al*, 2006). In some cases, this leads to no measurable *BOLD* signal despite evidence of neuronal activity (Rossini *et al*, 2004). Consequently, there is a need to critically evaluate the *BOLD* fMRI methodology in chronic stroke patients, and possibly develop more specific noninvasive imaging techniques.

It has been hypothesized that less widely utilized noninvasive fMRI techniques, for example, arterial spin labeling (ASL) (Williams *et al*, 1992), which is sensitive to changes in *CBF*, and vascular-space-occupancy (VASO) (Lu *et al*, 2003), which is sensitive to changes in *CBV*, might more accurately quantify details of cortical hemodynamics in chronic stroke (Donahue *et al*, 2012). Clinically, ASL has been used to show perfusion deficits in acute (MacIntosh *et al*, 2010*b*) and chronic (Brumm *et al*, 2010) stroke and VASO has been successfully applied in studies of ischemic steno-occlusive disease (Donahue *et al*, 2009*c*, 2010). However, no fMRI activation studies have directly compared *BOLD* with these new fMRI techniques, nor evaluated their feasibility or added value in chronic stroke. Here, we systematically evaluated *CBF*-weighted (*CBFw*), *CBV*-weighted (*CBVw*), and *BOLD* responses associated with a motor task in chronic stroke patients and age-matched controls. Our primary hypothesis was that *BOLD* fMRI would underestimate the area of cortical activity in stroke patients relative to separate weighted measures of *CBF* (as quantified using ASL) and *CBV* (using VASO). A secondary hypothesis was that differences between fMRI techniques would be more prevalent in patients with large-vessel disease, as these patients lack the ability to regulate *CBF* to the same extent as healthy subjects. Results establish the feasibility of performing multimodal fMRI in chronic stroke patients, demonstrate discord in hemodynamic coupling in patients, and outline the strengths and limitations of multimodal investigations in chronic stroke.

Materials and methods

All participants ($n = 22$) provided informed, written consent, and the study was carried out in accordance with local Research Ethics Committee approval (Oxfordshire Research Ethics Committee A Ref: 06/Q1604/2). Stroke patients ($n = 11$; age = 61 years ± 13) with motor impairment (Table 1) and age-matched controls ($n = 11$; age = 61 years ± 8, 6 males) with no history of cerebrovascular disease were enrolled. Stroke patients with residual hand paralysis, identified from discharge letters from a local rehabilitation clinic, were considered for participation if they had no prior history of neurological disease, but excluded if they had persistent complete paralysis of the hand or MRI contraindications. Based on hospital discharge letters and prior clinical imaging, evidence of atherosclerosis was documented. Patient motor deficits at enrollment were recorded using the upper extremity section from the Fugl-Meyer score scale (range 0 to 66) (Fugl-Meyer *et al*, 1975).

Magnetic Resonance Imaging

All participants were scanned at 3.0T (Siemens, Erlangen, Germany). *BOLD*-fMRI: Gradient-echo ($TE = 40/TR = 3,000$ milliseconds) with single-shot 2D echo planar imaging readout; spatial resolution = $3.8 \times 3.8 \times 3.8$ mm³. ASL and VASO: To assess *CBFw* and *CBVw* changes, ASL and VASO with FLuid Attenuated Inversion Recovery (VASO-FLAIR) were used, respectively (Donahue *et al*, 2009*a*; Gunther *et al*, 2005). Briefly, ASL measures *CBF* by magnetically tagging the longitudinal magnetization of blood water in inflowing arteries with a radiofrequency pulse and collecting an image after the tagged blood water reaches the capillaries. A control image without tagging is also collected and a subtraction of *control—tag* yields a *CBFw* image. The VASO sequence is sensitive to changes in *CBV*. This is achieved by adiabatically inverting all water magnetization within the body coil and collecting an image at an inversion time (*TI*) when the longitudinal magnetization of the blood water is zero. As water in blood and tissue have different recovery times (T_1), detectable tissue water signal is available at the time of blood water nulling. Thus, the VASO contrast is effectively extravascular. Reductions in the extravascular water signal associated with vasodilation can be measured, thus providing *CBVw* contrast from which *CBV* changes can be inferred. Cerebrospinal fluid fluctuations additionally contribute to the VASO contrast, and therefore a second inversion pulse was added to allow for simultaneous nulling of blood and cerebrospinal fluid water, an approach called VASO-FLAIR. A 3D GRadient And Spin Echo (GRASE) readout was used to collect whole-brain ASL and VASO-FLAIR images. The benefit of the single-shot 3D GRASE readout is constant ASL and VASO-FLAIR *TI* across slices, leading to equivalent transit time sensitivity (ASL) and blood water nulling (VASO-FLAIR) across the imaging volume (Donahue *et al*, 2009*a*).

Table 1 Patient characteristics

Case no.	Age (years)	Sex	Stroke type	Stroke location	Time since stroke (months)	Fugl-Meyer motor subscore (0–66)	Risk factors and vessel occlusion
1	69	M	Infarct	Left PCA	9	59	15% Bilateral ICA stenosis. History of diabetes, hypertension, and high cholesterol
2	44	M	Infarct	Left MCA	23	64	History of smoking, high cholesterol, and hypertension. CT-angio showed normal vessels from the CCA to Circle of Willis
3	57	M	Hemorrhage	Left intracerebral	49	50	Hypertension, high cholesterol, and over weight
4	65	M	Infarct	Right subcortical	18	64	No ICA/CCA stenosis Smoked before stroke
5[†]	66	M	Infarct	Right MCA	11	56	Complete right ICA occlusion, no surgery History of hypertension, smoked before stroke
6[†]	29	F	Infarct	Right MCA	30	59	Right carotid artery dissection. Persistent occlusion of right carotid artery
7[*]	72	M	Infarct	Right MCA	41	61	Smoking, hypertension No info on carotid Doppler
8	61	M	Infarct	Right MCA	26	37	25% Stenosis right CCA, 25% left ICA, 15% right ICA History of hyperlipidemia
9[†]	77	F	Infarct	Left MCA	39	34	80% Stenosis left ICA. Prior left carotid endarterectomy History of hypertension, hypercholesterolemia
10[†]	71	M	Infarct	Left MCA and ACA	44	51	Bilateral ICA stenosis >85%, no surgery History of hypertension
11[†*]	61	M	Ischemia	Cortical ACA	57	64	Bilateral ICA occlusion, no surgery

ACA, anterior cerebral artery; CCA, common carotid artery; CT, computed tomography; ICA, internal carotid artery; MCA, middle cerebral artery; PCA, posterior cerebral artery.
*Coregistration not possible. †Large vessel disease and possibly decreased vascular reserve capacity.

Sequence-specific parameters were ASL 3D GRASE: pulsed ASL with background suppression, $TR/TI = 2{,}500/1{,}600$; VASO-FLAIR 3D GRASE: $TR/TI1/TI2 = 5{,}000/2{,}256/737$ milliseconds. Note that the effective TR of the ASL difference images was therefore 5,000 milliseconds. All scans used a matched spatial resolution $= 3.8 \times 3.8 \times 3.8$ mm³. T_1-weighted structural images ($1 \times 1 \times 1$ mm³) were acquired for coregistration purposes.

Functional Paradigm

During fMRI (*BOLD*, VASO-FLAIR, and ASL) a custom-made wooden joystick was used, which allowed for isolated wrist extension–flexion movement. Scan order was randomized and participants performed 1 Hz wrist extension/flexion in four blocks of 60 seconds/30 seconds rest/movement, followed by an additional 60 seconds of baseline rest at the end of the experiment. Movements were visually cued by an asterisk moving laterally at 1 Hz. Patients performed the movement using the affected hand (contralateral to affected brain hemisphere) and healthy subjects used their dominant hand.

Postprocessing

Functional MRI data were corrected for motion and baseline drift and linear coregistration to T_1-weighted images and subsequently to 2 mm MNI (Montreal Neurological Institute) standard space was performed (Jenkinson and Smith, 2001). In two subjects with large existing infarcts as well as noticeable bulk head motion (Pts 7, 11), coregistration was not possible and these volunteers were excluded from analysis. Whole-brain fMRI time series data were analyzed using custom Matlab scripts. Unthresholded positive mean subject z-statistic maps for the contrast of movement versus baseline were recorded. Individual subject signal change and reactivity values, and signal time courses, were extracted from an anatomical region of interest (ROI). Primary motor cortex *M1* was chosen as an ROI (Brodmann area 4) in the hemisphere contralateral to the moved hand, as defined by the Jülich Histological Atlas, which was linearly transformed in the same MNI space as the coregistered fMRI data (Eickhoff et al, 2005). Within the ROI, the mean *BOLD*, *CBFw*, and *CBVw* reactivity were calculated separately for healthy subjects and patients. This procedure of using an anatomical ROI was chosen so as not to bias the signal change calculations by different statistical reactivity from any one of the fMRI scans.

Statistical Analysis

As the *BOLD*, *CBFw* ASL, and *CBVw* VASO-FLAIR signal changes were calculated within an anatomical ROI rather than from statistical activation maps, we formally evaluated the statistical significance of the activation on both a subject-specific basis and using the group averaged time courses from each fMRI modality. The first three time points (9 seconds; *BOLD*) or one time point (5 seconds; ASL and VASO-FLAIR) of the activated period were not included

to allow for the signal to plateau; these numbers differ slightly owing to the difference in *TR* between *BOLD* (*TR* = 3 seconds) and ASL and VASO-FLAIR (*TR* = 5 seconds) and knowledge that changes in *CBF* and *CBV* slightly precede *BOLD* changes. For baseline, 30 seconds (*BOLD*, ASL, and VASO-FLAIR) after the end of the joystick movement were excluded to allow for *CBF* and *CBV*, and a possible *BOLD* poststimulus undershoot, to return to baseline. The first 33 seconds (*BOLD*) and 35 seconds (ASL and VASO-FLAIR) of data were also not used for baseline correction, to allow for signal to reach steady state. This resulted in the baseline (*BOLD*: $n_1 = 49$; ASL and VASO-FLAIR: $n_1 = 29$) and activated (*BOLD*: $n_2 = 28$; ASL and VASO-FLAIR: $n_2 = 20$) time points being unequal. The sample size using the above time points was determined to be large enough to support a normal distribution approximation, and the difference between epochs is reported with the *z*-statistic and corresponding two-tailed *P* value. Owing to the relatively sparse temporal sampling, which also differed between *BOLD* (*TR* = 3 seconds) and ASL/VASO-FLAIR (*TR* = 5 seconds), it was determined that the data were not sufficient to reliably report additional metrics such as onset time and time-to-peak and therefore the focus of this study was on mean signal changes.

Interpreting Cerebral Blood Flow-Weighted Arterial Spin Labeling and Cerebral Blood Volume-Weighted Vascular-Space-Occupancy FLuid Attenuated Inversion Recovery Contrast

It is possible to estimate changes in *CBF* from the relative ASL signal changes (Donahue *et al*, 2009*a*; Kim *et al*, 2012); however, it is frequently assumed in functional ASL experiments that the ASL signal change is a direct indicator of changes in *CBF*. This assumption is an oversimplification as both *CBF* and arterial transit time (*ATT*) change with activation, which collectively influence the ASL contrast in a manner that depends on postlabeling delay (*TI*). In principle, one can quantify both the *CBF* and *ATT* by performing an ASL experiment at multiple postlabeling delays. Using this approach with a comparable motor stimulus, it has been demonstrated that the *ATT* reduction is approximately equal to the *CBF* increase (Gonzalez-At *et al*, 2000). In clinical studies, multiple postlabeling delay acquisitions lead to long scan times and poor task compliance from the patients, and therefore assumptions are generally made regarding how the *ATT* and absolute *CBF* changes can be interpreted, ideally within a range of possible scenarios. To understand this, we simulated ASL kinetic curves using the solution to the single-compartment flow-modified Bloch equation (Zhou and van Zijl, 1999) accounting for different physiologically plausible changes in *CBF* and *ATT*.

$$\Delta M_{\text{tissue}}(TI)$$
$$= \begin{cases} 0 & TI < \tau_a \\ 2\alpha M_0 c \left[e^{-TI/T_{1,a}} - e^{-\tau_a/T_{1,a}} e^{-(TI-\tau_a)/T_{1,\text{app}}} \right] & \tau_a \leq TI < \tau_d \\ 2\alpha M_0 c \left[e^{-\tau_d/T_{1,a}} e^{-(TI-\tau_d)/T_{1,\text{app}}} - e^{-\tau_a/T_{1,a}} e^{-(TI-\tau_a)/T_{1,\text{app}}} \right] & \tau_d \leq TI \end{cases}$$
$$\tag{1}$$

where $1/T_{1,\text{app}} = 1/T_{1,\text{GM}} + f/\lambda$, $c = (f/\lambda)(1/T_{1,\text{app}} - 1/T_{1,a})^{-1}$, f is the *CBF* (mL per gram per milliseconds), M_0 is the equilibrium magnetization of blood water, $\alpha \approx 1$ is the inversion efficiency, $\tau_a \approx 600$ milliseconds and $\tau_d \approx 1,500$ milliseconds are the times for the leading and trailing edge of the bolus in motor cortex, respectively (Gallichan and Jezzard, 2009; MacIntosh *et al*, 2010*a*), $T_{1,\text{GM}} \approx 1,200$ milliseconds (Lu *et al*, 2005) and $T_{1,a} \approx 1,600$ milliseconds (Lu *et al*, 2004) are the tissue and arterial blood water T_1, respectively, and $\lambda \approx 0.9$ mL blood/g brain is the whole-brain blood/tissue water partition coefficient (Herscovitch and Raichle, 1985). Upon stimulation, the *CBF* will increase, and the *ATT* has been shown to reduce by approximately an equal amount (Gonzalez-At *et al*, 2000). Note that the *ATT* reduction should reduce both the τ_a and τ_d terms equally.

For VASO-FLAIR, the *CBV* quantification procedure has been outlined previously (Donahue *et al*, 2006); however, the salient aspects of this procedure and required assumptions are briefly reproduced here. The signal in the VASO-FLAIR experiment can be written,

$$S_{\text{GM}}^i \sim \left(C_{\text{GM}} - CBV_{\text{GM}}^i \cdot C_b \right) \cdot M_{z,\text{GM}}$$
$$\cdot e^{-TE/T_{2,\text{GM}}^i} \text{ for } i = \text{(act)ivation or (base)line} \tag{2}$$

where $C_{\text{GM}} = 0.89$ mL water/mL gray matter and $C_b = 0.87$ mL water/mL blood are the gray matter parenchyma and blood water densities, respectively (Donahue *et al*, 2006); CBV_{GM} is the gray matter parenchymal *CBV*, $TE = 40$ milliseconds is the echo time, $T_{2,\text{GM}}^{\text{base}} = 70.8$ milliseconds and $T_{2,\text{GM}}^{\text{act}} = 71.4$ milliseconds are the transverse relaxation times of gray matter at 3.0T as measured previously (Donahue *et al*, 2006), and $M_{z,\text{GM}}$ is the longitudinal magnetization of blood water in the steady-state double inversion recovery VASO-FLAIR experiment,

$$M_{z,\text{GM}} = 1 - \left[2 - (2 - e^{-(TR-TI1-TI2)}) \cdot e^{-TI1/T_{1,\text{GM}}} \right] \cdot e^{-TI2/T_{1,\text{GM}}}$$
$$\tag{3}$$

where $TI1 = 2,256$ milliseconds is the spacing between the first and second inversion pulse, $TI2 = 737$ milliseconds is the spacing between the second inversion pulse and the excitation pulse, and $TR = 5,000$ milliseconds. In this model, we have neglected the effect of exchange and fresh blood water inflow, which have both been shown to be small at $TR = 5,000$ milliseconds (Donahue *et al*, 2006, 2009*b*). Finally, the *CBV* change can be estimated from the measured signal change,

$$\frac{S_{\text{GM}}^{\text{act}} - S_{\text{GM}}^{\text{base}}}{S_{\text{GM}}^{\text{base}}} = \frac{\Delta S_{\text{GM}}}{S_{\text{GM}}^{\text{base}}} \tag{4}$$

to give:

$$CBV_{\text{GM}}^{\text{act}}$$
$$= \frac{C_{\text{GM}} - (\Delta S_{\text{GM}}/S_{\text{GM}} + 1)(C_{\text{GM}} - CBV_{\text{GM}}^{\text{base}} \cdot C_b)e^{TE\left(1/T_{2,\text{GM}}^{\text{act}} - 1/T_{2,\text{GM}}^{\text{base}}\right)}}{C_b}$$
$$\tag{5}$$

The only remaining unknown in equation (5) is $CBV_{\text{GM}}^{\text{base}}$, which must be assumed when translating VASO-FLAIR

signal changes to absolute *CBV* changes. Here, we have assumed $CBV_{GM}^{base} = 0.05 \, mL/mL$, consistent with literature values (Grandin *et al*, 2005; Leenders *et al*, 1990); however, this value could differ between individuals and voxels. Therefore, caution should be taken in interpreting the VASO-FLAIR signal changes in terms of absolute *CBV* changes. Rather, we propose that the *CBVw* VASO-FLAIR responses should be interpreted broadly in terms of directional relationships and in the context of the *BOLD* and ASL signal changes.

Results

When the average fMRI responses were considered, all three fMRI modalities showed significant changes within the *M1* ROI of healthy subjects ($P < 0.01$) (Table 2). Signal changes corresponded to a relative increase in *BOLD* = 0.3% ± 0.1%, *CBFw* = 20% ± 4%, and *CBVw* = 16% ± 5%. The VASO-FLAIR data were determined to be least robust on a single-subject basis, with several subjects eliciting nonstatistically significant changes (see Supplementary Material). In stroke patients, *BOLD* fMRI yielded no significant changes on average (*BOLD* = 0.1% ± 0.4%) within *M1* ($P = 0.20$), despite significant changes in *CBFw* = 15% ± 7% ($P < 0.01$) and *CBVw* = 14% ± 9% ($P < 0.01$). Although larger average increases in *CBFw* and *CBVw* were seen in controls relative to patients, these differences were not significant (Figure 1B; *CBFw*, $P = 0.36$; *CBVw*, $P = 0.25$).

Inspection of individual volunteer data revealed additional information regarding underlying patterns of change. For instance, Figure 2 shows reactivity from a representative control volunteer (Figure 2A). By contrast, a range of patterns was observed in patients, including positive (Figure 2B), negative (Figure 2C), and absent (Figure 2D) *BOLD* changes. The *BOLD* dynamics are directionally consistent with the corresponding changes in *CBF* and *CBV* (Table 3). Inspection of the *BOLD* time course of each patient demonstrated positive *BOLD* signal in patients 2, 3, 4, 5, 6, and 9, a negative *BOLD* signal in patient 8, and undetectable *BOLD* change in the remaining patients (see Supplementary Material). Thus, joystick-related *BOLD* signal changes were absent in patients with and without known large-vessel disease (Table 1). Motor Fugl-Meyer scores

Table 2 Control and patient mean reactivity

	ΔBOLD %	*ΔCBFw* %	*ΔCBVw* %
M1 region of interest			
Controls	0.3 ± 0.1	20 ± 4	16 ± 5
Patients	0.1 ± 0.4	15 ± 7	14 ± 9

BOLD, blood oxygenation level-dependent; CBFw, cerebral blood flow-weighted; CBVw, cerebral blood volume-weighted.
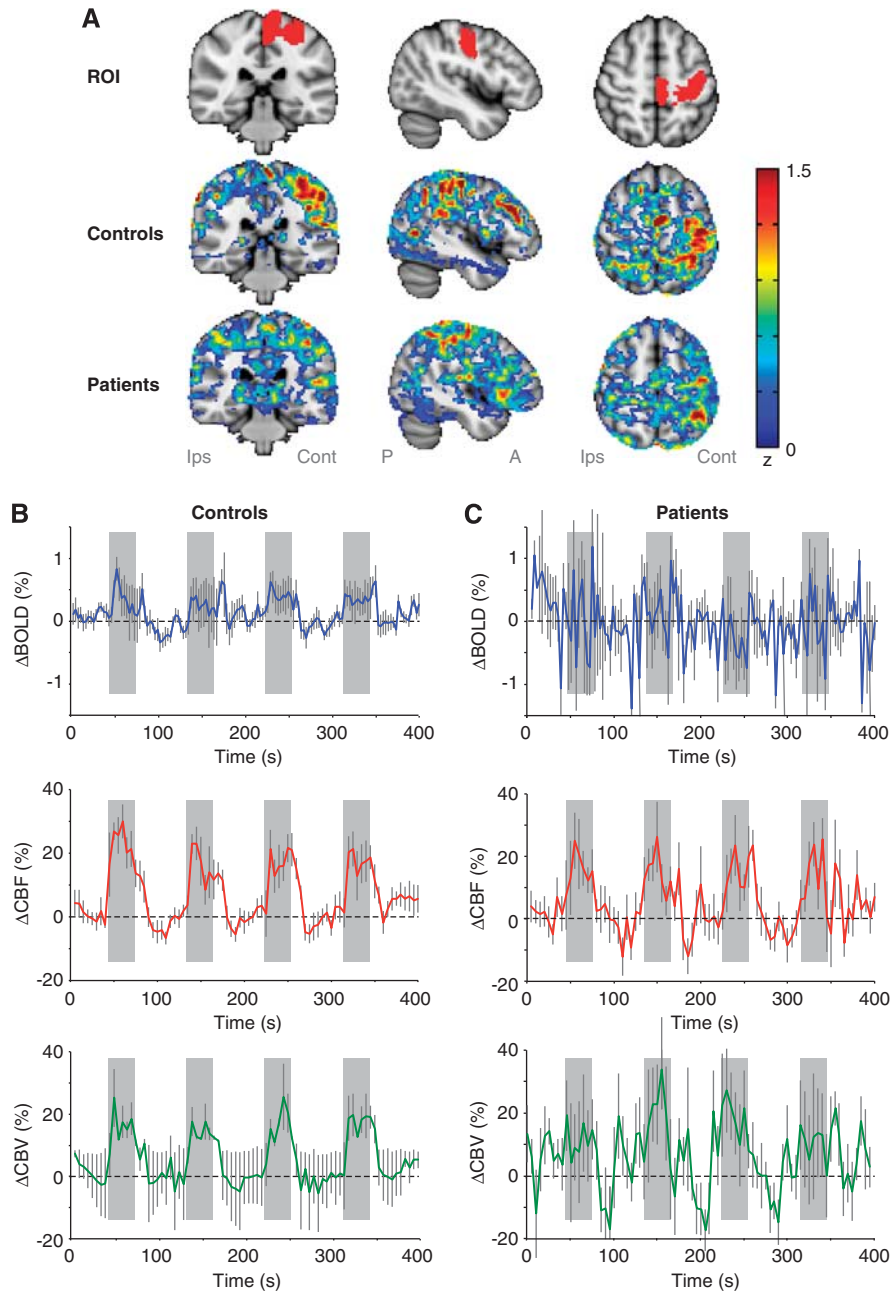Mean signal changes in patients and controls (see Supplementary material for individual subject changes).

were comparable between patients with a positive *BOLD* signal and patients with no or negative *BOLD* responses (mean 54.5 versus 54.4; $P > 0.05$; see Table 1).

Additionally, we evaluated reactivity measures in the contralateral hemisphere to impairment (ipsilateral to joystick movement). As can be seen from the unthresholded positive z-maps in Figure 1A, the patient *BOLD* reactivity is much more homogeneous across right and left hemispheres than is the control reactivity. When the anatomical ROI (Figure 1A) is mirrored to the opposite hemisphere, the following signal changes were found for controls: *BOLD* = 0.16% ± 0.15%, *CBFw* = 19% ± 3% and *CBVw* = 8% ± 3%; and for patients: *BOLD* = −0.04% ± 0.3%, *CBFw* = 13% ± 5% and *CBVw* = 22% ± 6%. However, these responses were at or below the noise level in the majority of subjects.

The *CBFw* signal can be interpreted in the context of different physiological changes in *CBF* and *ATT*, as outlined in Figure 3. As can be seen, for long postlabeling delay > 1,500 milliseconds, the ASL contrast is less sensitive to *ATT*. In this regime, where our experiments are performed, normalized changes in $\Delta M/M_0$ are shown for *CBF* and *ATT* changes of 15%, 24%, and 33%. The mean change in ASL signal observed here ($\sim 20\%$) is roughly consistent with a slightly larger increase in *CBF* ($\sim 24\%$) and a reduction in *ATT* ($\sim -24\%$) with stimulation, however, as described above the precise values will depend on the magnitude of the change in *ATT*.

Discussion

This study demonstrates that in chronic stroke, motor activity was associated with increases in *CBF* and *CBV* in primary motor cortex despite no measurable *BOLD* fMRI response. Blood oxygenation level-dependent fMRI may therefore be of limited value as a surrogate measure of cortical activation patterns in the course of rehabilitation. While this has been hypothesized in earlier studies, to our knowledge this is the first demonstration that alternative fMRI approaches provide interpretable hemodynamic information in the absence of *BOLD* changes in chronic stroke patients. This could indicate that ASL- and possibly VASO-based fMRI may be superior to *BOLD* fMRI when investigating poststroke cortical activation patterns. Importantly, when averaging reactivity across patients there is no coherent group behavior, yet trends on an individual subject basis are apparent, thereby suggesting that such multimodal imaging may be useful for understanding stages of impairment.

Hemometabolic Uncoupling

Blood oxygenation level-dependent fMRI is sensitive to changes in the amount of deoxygenated hemo-

Figure 1 (**A**) The anatomical region of interest (ROI) used for all control and patient volunteers, as well as the separate unthresholded *z*-stats for the control and patient volunteers. Note that the *z*-stats are highly asymmetric for the control volunteers, as expected for the unilateral joystick task, however, are smaller and more evenly distributed between cortices for the patients. Average (**B**) control and (**C**) patient blood oxygenation level-dependent (*BOLD*), cerebral blood flow-weighted (*CBFw*), and cerebral blood volume-weighted (*CBVw*) reactivity time courses within *M1*. Gray blocks correspond to stimulus periods and error bars represent standard error over all volunteers in each group. Note the absence of a mean *BOLD* signal change in patients, yet clear *CBFw* and *CBVw* reactivity, thereby suggesting discord in *CBF*, *CBV*, and cerebral metabolic rate of oxygen consumption (*CMRO$_2$*) coupling relationships following chronic stroke, unclear from *BOLD* measurements alone.

globin in the brain. Consequently, changes in *CBF*, *CBV*, and *CMRO$_2$* all affect the *BOLD* signal. In healthy subjects, the change in *BOLD* signal during functional hyperemia relies on a decrease in oxygen extraction fraction (Raichle and Mintun, 2006), and thus a decrease in the amount of paramagnetic (*BOLD*-weighted MR signal reducing) deoxygenated

hemoglobin. In stroke patients, however, baseline *CBF* and *CBV* and impaired vascular reserve capacity may alter these hemodynamic changes (Mandell *et al*, 2008). Underlying atherosclerosis, which causes $\sim 25\%$ of all ischemic strokes (Mustanoja *et al*, 2011), has been shown to decrease both baseline *CBF* (Brumm *et al*, 2010) and vascular reserve
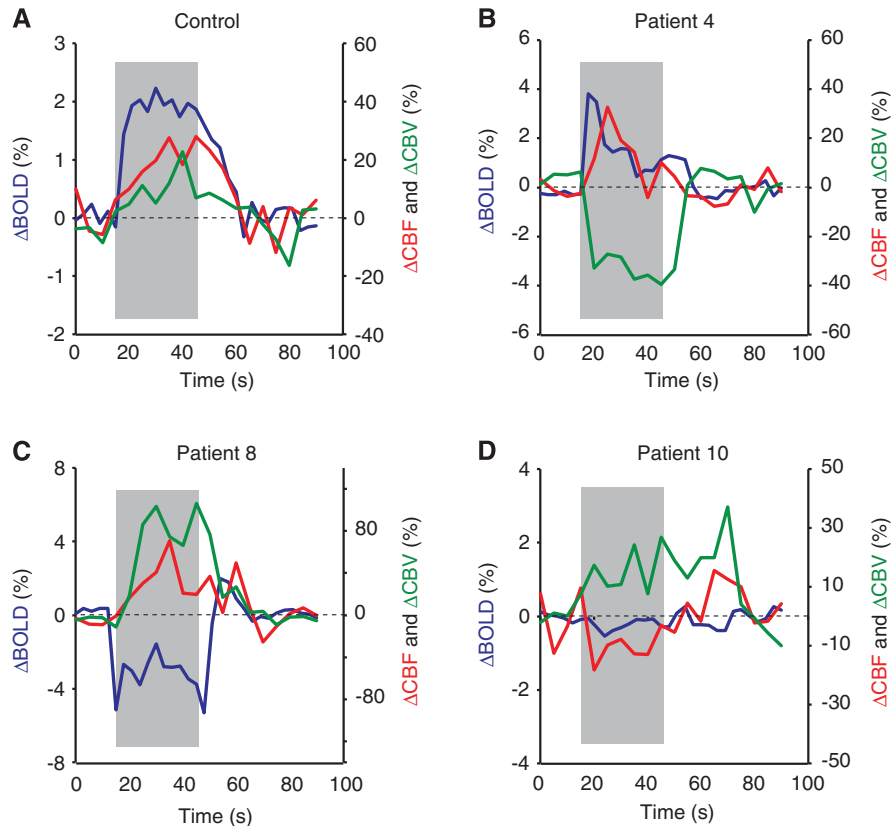
Figure 2 Representative block-averaged time courses for (**A**) a control subject and (**B**–**D**) three patients. Gray areas depict the stimulus period. For the control, a robust blood oxygenation level-dependent (*BOLD*) change ($P < 0.05$) is observed with normal cerebral blood flow-weighted (*CBFw*) ($P < 0.05$) and cerebral blood volume-weighted (*CBVw*) ($P < 0.05$) reactivity. Alternatively, the patients show a more complex array of variation. (**B**) A small, positive *BOLD* change ($P < 0.05$) is explained by a small *CBFw* increase ($P < 0.05$) and negative *CBVw* change ($P < 0.05$), implying possible vascular steal in the region. (**C**) A negative *BOLD* change ($P < 0.05$) is explained by a large *CBVw* increase ($P < 0.05$), consistent with vasodilatory autoregulation, and a smaller *CBFw* change ($P < 0.05$). (**D**) A patient with effectively no *BOLD* ($P > 0.05$) and near-negligible *CBFw* change ($P < 0.05$), yet small vasodilatory *CBVw* change ($P < 0.05$). Importantly, patients display a more complex array of hemometabolic coupling relationships, which require independent estimations of *CBF* and *CBV* to understand fully.

Table 3 Different possibilities for observing positive (above) and negative (below) BOLD responses

	ΔCBF	*ΔCBV*	*ΔCMRO$_2$*	*BOLD*
Positive BOLD response				
Healthy coupling	+++	+	+	+++
(Minor) autoregulation	+++	++	+	++
Negative BOLD response				
(Severe) autoregulation	+++	+++	+	−
Vascular steal	−	−	None	−
Stroke with compliant vasculature	+	+++	+	−
Stroke with noncompliant vasculature	None	None	+	−

BOLD, blood oxygenation level-dependent; CBF, cerebral blood flow; CBV, cerebral blood volume; CMRO$_2$, cerebral metabolic rate of oxygen.
Positive change (+), negative change (−), no change (none). Additional symbols denote smaller or larger relative changes (to healthy coupling) in the given direction. The magnitude of these relationships will depend heavily on the extent of the impairment of each of the parameters involved; this table is intended only as a guide for explaining possible positive and negative *BOLD* changes in different stages of stroke. Understanding the precise mechanism of impairment requires independent measures of *CBF*, *CBV*, and *CMRO$_2$*.

capacity (Mandell *et al*, 2008), while increasing baseline *CBV* (Derdeyn *et al*, 2002). As a consequence of these changes in hemodynamics, neuronal activity is not necessarily coupled to regional *CBF* and *CBV* changes to the same degree as in healthy subjects. Rossini *et al* (2004) performed a combined
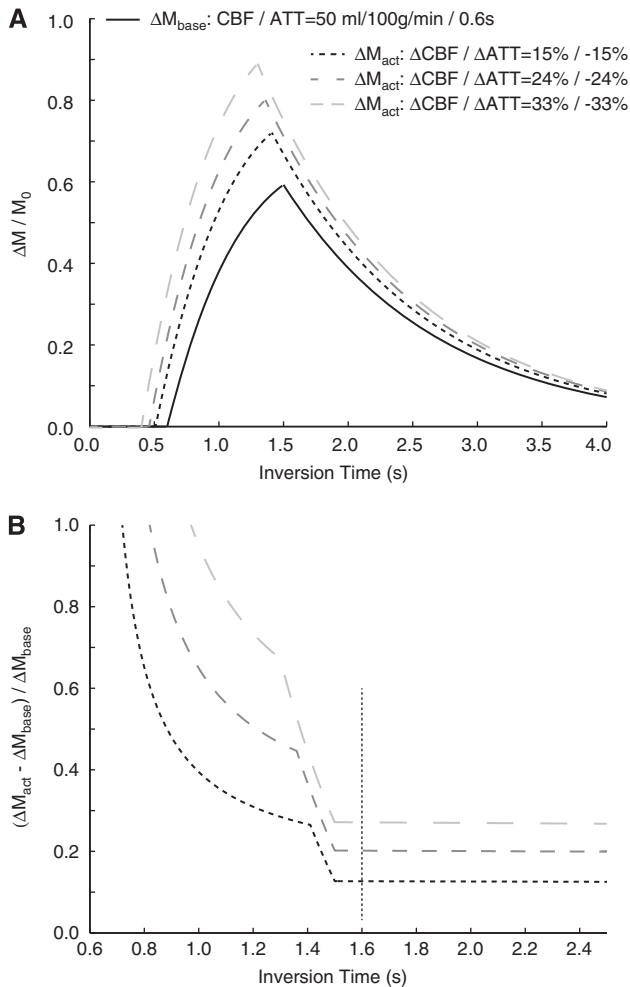
Figure 3 (**A**) Arterial spin labeling (ASL) kinetic curves for a baseline cerebral blood flow (*CBF*) = 50 mL/100 g per minute and arterial transit time (*ATT*) = 0.6 seconds and different possibilities from changes in these parameters during motor stimulation. Here, the increase in *CBF* has been taken to be equal to the reduction in *ATT*, and three scenarios for changes of 15%, 24%, and 33% are shown. (**B**) The change in ASL difference magnetization (normalized by baseline ASL difference magnetization), for the three activation scenarios in (**A**). Note that at short inversion time (*TI*), the reactivity measures depend heavily on choice of *TI*, yet at longer *TI*, the contrast is less sensitive to this parameter. These plots provide an exemplar for interpreting the cerebral blood flow-weighted (*CBFw*) changes in terms of absolute changes in *CBF* and *ATT*.

BOLD fMRI and MEG study, in which they showed that, although electrical stimulation of the median nerve led to clear MEG signals in stroke patients, some patients showed no measurable *BOLD* fMRI signal. Previous *BOLD* fMRI stroke studies have found transiently missing *BOLD* signal (Binkofski and Seitz, 2004), a lower *BOLD* signal change compared with healthy subjects in both affected (Newton *et al*, 2002) and unaffected (Pineiro *et al*, 2002) hemispheres, and patterns of persistent recruitment of ipsilateral activity or slow recovery to more localized contralateral *BOLD* activity (Feydy *et al*,

2002). However, a recent review failed to find a consistent correlation between imaging findings and clinical improvement during poststroke recovery (Buma *et al*, 2010).

The current study expands on literature findings by demonstrating that novel fMRI techniques sensitive to *CBF* and *CBV* changes are feasible in this patient group and may be more sensitive than the *BOLD* technique in patients with abnormal neurovascular coupling (*CMRO*$_2$ changes relative to those of *CBF* and *CBV*). These results show that regional activity-induced *CBF* and *CBV* increases tended to be lower in patients than in healthy subjects and that this coincides with the absence of significant *BOLD* signal increase. This could be explained by a partially occluded vessel delivering exactly the amount of oxygen needed to satisfy the increase in *CMRO*$_2$ (due to no change in deoxygenated hemoglobin). However, patients without significant large-vessel disease (e.g., Patient 1) also showed impaired *BOLD* signal, and patients with persistent ICA occlusion (e.g., Patient 6) or previous ICA surgery due to known large-vessel disease (e.g., Patient 9) showed a positive *BOLD* signal. Previous studies have also shown impaired vascular reserve capacity in patients with suspected small-vessel disease due to hypertension (Ficzere *et al*, 1997), as well as lower *BOLD* response in patients with lacunar strokes (Pineiro *et al*, 2002) and/or white matter degeneration (Hund-Georgiadis *et al*, 2003), arguing in favor of an impairment of *BOLD* reactivity in both large- and small-vessel disease.

Experimental Limitations and Concerns of Multimodal Functional Magnetic Resonance Imaging in Stroke Patients

In the interest of time, we used an ASL technique with a single identical labeling delay for all participants as is commonly performed in functional ASL studies. This may have biased the quantitative *CBF* since some patients may have had prolonged *ATT*. Also, while patient performance was monitored, variability in performance and possible mirror movements could confound results.

Motion is always a concern in fMRI experiments, especially when patients are involved, and we took precautions to reduce the effect of this possible complication. First, extensive padding and hook and loop fastners were used to secure the head within the coil and all volunteers were reminded of the importance of remaining still throughout the experiment. Second, affine motion correction routines were applied as outlined. Subsequently, all data were inspected to determine if poor coregistration and/or excessive motion precluded further analysis and this was found to be the case in two of the 11 patients (18% of patients or 9% of all volunteers). We critically reviewed all data to understand the role that motion may play in the analysis. We found two

2052

types of motion that are of potential interest. First, bulk head motion was largely minimal in the volunteers included in the study (omitting the two described above). This bulk head motion is potentially most relevant as a complicating issue as it could coincide with the movement of the joystick. However, we did not observe this to be any more prevalent in patients than controls, nor between previous fMRI studies conducted in our research center (Donahue *et al*, 2009a). The second type of motion was motion of the tissue within the skull, which we believe is derived from small changes in tissue position during pulsations of blood through vasculature. This sort of motion appeared to be more pronounced in the patients relative to the controls, likely owing to increased tissue atrophy and reduced tissue rigidity. These fluctuations occur at a much higher frequency than bulk head motion, and may provide some explanation for the increased frequency fluctuations in the patients relative to the controls. However, these fluctuations largely appear as relatively constant high-frequency fluctuations and do not correlate with the stimulus epochs. Additionally, the directional relationships of changes in *BOLD*, *CBFw*, and *CBVw* responses are largely consistent in terms of what is expected physiologically and thus we do not believe this motion is the dominant effect seen in our data. Finally, to reduce the confound of differences in coregistration performance between subjects, we chose a relatively large anatomical ROI to analyze our data. Therefore, this approach is less sensitive to coregistration than an approach where a much smaller ROI would be chosen. We cannot rule out the possibility of motion contributing to the time courses, and indeed we believe that there are some confounds related to this as there likely are in most clinical fMRI experiments. However, we took several precautions to reduce complications from motion and coregistration and we believe that the dominant effects reported in the data are not derived from motion. Related to these observations, we do stress that the time of the multimodal experiments (21 minutes total) is at the limit of compliance for many patients, and future experiments would benefit from reducing the duration of the paradigm.

In theory, an absent *BOLD* response could be due to patients not performing the task as instructed, or due to increased involvement of other cortical areas than *M1*. However, the fact that ASL and VASO-FLAIR showed significant activation within *M1*, despite these techniques having lower SNR than *BOLD*, indicates that *M1* is most likely metabolically active during task performance. However, despite the fact that ASL- and VASO-FLAIR fMRI show activation in areas without *BOLD* response, there is no guarantee that these techniques are of greater value when explaining impairment or recovery. Both ASL and VASO-FLAIR also rely on a coupling between neuronal activity and hemodynamic changes, and thus suffer from some of the same constraints as

BOLD, but arguably to a lesser degree. Consequently, techniques more directly sensitive to changes in $CMRO_2$ will be beneficial. Finally, *BOLD*, ASL, and VASO-FLAIR experiments were performed sequentially, and therefore variations in performance between scans could confound interpretation. However, scan order was randomized between patients and controls, therefore the absence of a *BOLD* response at the group level is likely not due to a bias from scan order or habituation.

In the present study, we investigated changes in primary motor cortex only. However, previous studies in patients with cerebral microangiopathy or untreated hypertension have shown impaired *BOLD/CBF* response in the parietal lobe and thalamus, suggesting that neurovascular coupling is disturbed beyond primary motor cortex. For evoked multimodal experiments, strong motor and/or visual stimuli are generally used, owing to the ability to elicit changes in distinct cortical regions in a controlled and robust manner. However, Poser and Norris (2011) have more recently demonstrated that additional brain regions can be studied using ASL and VASO, and we have recently implemented VASO to study *CBV* changes in hippocampus and fusiform gyrus in patients with memory disorders. Largely owing to contributions from intravascular signal and relatively low SNR, ASL, and VASO remain problematic in very low brain regions such as brainstem and cerebellum; however, we anticipate that other regions of cerebrum could easily be assessed given an appropriate choice of stimuli.

Recently, *BOLD* MRI in combination with a vascular challenge (i.e., elevated CO_2 inhalation) has been suggested as a tool to evaluate cerebrovascular reactivity, and a useful technique in presurgical evaluation of patients with steno-occlusive disease. However, a recent study by Mandell *et al* (2008) compared *BOLD* and ASL measures of cerebrovascular reactivity and found only moderate agreement between the techniques, despite the fact that all participating patients had large-vessel stenosis or occlusion. Importantly, hypercarbia will elicit global cortical changes in *CBF* and *CBV*, with minimal changes in $CMRO_2$. Therefore, this task could be more specifically used to look at cerebrovascular reactivity rather than vascular and metabolic activity secondary to neuronal stimulation as in the present study. The major limitation of only using *BOLD* in vascular reactivity measurements is that the *BOLD* effect will report on ensemble changes in *CBF* and venous *CBV* (and to a smaller extent arterial *CBV*). Application of ASL and VASO will provide a more direct measure of the vascular phenomena underlying the *BOLD* reactivity and whether *CBF* and *CBV* are disproportionately impaired. Additionally, these data could be useful for better understanding ambiguous *BOLD* effects, such as negative *BOLD* effects frequently attributed to 'vascular steal.' By separately measuring *CBFw* and *CBVw* reactivity, it should be possible to more precisely understand the changes

that are occurring in vasodilation (or vasoconstriction) and the corresponding flow response.

In conclusion, in patients with cerebrovascular disease it is difficult to infer changes in *CBF*, *CBV*, and neuronal activity based on *BOLD* signal changes alone. We performed multimodal, noninvasive fMRI in chronic stroke patients with motor impairments and demonstrated high variability in patient *BOLD* responses, yet more consistent and robust *CBF*, and to a lesser degree, *CBV* responses. Owing to the large and frequently unknown variability in neurovascular coupling that exists in chronic stroke, such multimodal fMRI approaches may be better suited than *BOLD* fMRI performed in isolation when interrogating cortical reorganization.

Acknowledgements

Disclosure/conflict of interest

References

Binkofski F, Seitz RJ (2004) Modulation of the BOLD-response in early recovery from sensorimotor stroke. *Neurology* 63:1223–9

Brumm KP, Perthen JE, Liu TT, Haist F, Ayalon L, Love T (2010) An arterial spin labeling investigation of cerebral blood flow deficits in chronic stroke survivors. *Neuroimage* 51:995–1005

Buma FE, Lindeman E, Ramsey NF, Kwakkel G (2010) Functional neuroimaging studies of early upper limb recovery after stroke: a systematic review of the literature. *Neurorehabil Neural Repair* 24:589–608

Cheeran B, Cohen L, Dobkin B, Ford G, Greenwood R, Howard D, Husain M, Macleod M, Nudo R, Rothwell J, Rudd A, Teo J, Ward N, Wolf S (2009) The future of restorative neurosciences in stroke: driving the translational research pipeline from basic science to rehabilitation of people after stroke. *Neurorehabil Neural Repair* 23:97–107

Derdeyn CP, Videen TO, Yundt KD, Fritsch SM, Carpenter DA, Grubb RL, Powers WJ (2002) Variability of cerebral blood volume and oxygen extraction: stages of cerebral haemodynamic impairment revisited. *Brain* 125: 595–607

Donahue MJ, Lu H, Jones CK, Edden RA, Pekar JJ, van Zijl PC (2006) Theoretical and experimental investigation of the VASO contrast mechanism. *Magn Reson Med* 56: 1261–73

Donahue MJ, Blicher JU, Ostergaard L, Feinberg DA, MacIntosh BJ, Miller KL, Gunther M, Jezzard P (2009*a*) Cerebral blood flow, blood volume, and oxygen metabolism dynamics in human visual and motor cortex as measured by whole-brain multi-modal magnetic resonance imaging. *J Cereb Blood Flow Metab* 29:1856–66

Donahue MJ, Hua J, Pekar JJ, van Zijl PC (2009*b*) Effect of inflow of fresh blood on vascular-space-occupancy (VASO) contrast. *Magn Reson Med* 61:473–80

Donahue MJ, van Laar PJ, van Zijl PC, Stevens RD, Hendrikse J (2009*c*) Vascular space occupancy (VASO) cerebral blood volume-weighted MRI identifies hemodynamic impairment in patients with carotid artery disease. *J Magn Reson Imaging* 29:718–24

Donahue MJ, Sideso E, MacIntosh BJ, Kennedy J, Handa A, Jezzard P (2010) Absolute arterial cerebral blood volume quantification using inflow vascular-space-occupancy with dynamic subtraction magnetic resonance imaging. *J Cereb Blood Flow Metab* 30:1329–42

Donahue MJ, Strother MK, Hendrikse J (2012) Novel MRI approaches for assessing cerebral hemodynamics in ischemic cerebrovascular disease. *Stroke* 43:903–15

Duncan PW, Lai SM, Keighley J (2000) Defining post-stroke recovery: implications for design and interpretation of drug trials. *Neuropharmacology* 39:835–41

Eickhoff SB, Stephan KE, Mohlberg H, Grefkes C, Fink GR, Amunts K, Zilles K (2005) A new SPM toolbox for combining probabilistic cytoarchitectonic maps and functional imaging data. *Neuroimage* 25:1325–35

Feydy A, Carlier R, Roby-Brami A, Bussel B, Cazalis F, Pierot L, Burnod Y, Maier MA (2002) Longitudinal study of motor recovery after stroke: recruitment and focusing of brain activation. *Stroke* 33:1610–7

Ficzere A, Valikovics A, Fulesdi B, Juhasz A, Czuriga I, Csiba L (1997) Cerebrovascular reactivity in hypertensive patients: a transcranial Doppler study. *J Clin Ultrasound* 25:383–9

Fugl-Meyer AR, Jaasko L, Leyman I, Olsson S, Steglind S (1975) The post-stroke hemiplegic patient. 1. A method for evaluation of physical performance. *Scand J Rehabil Med* 7:13–31

Gallichan D, Jezzard P (2009) Variation in the shape of pulsed arterial spin labeling kinetic curves across the healthy human brain and its implications for CBF quantification. *Magn Reson Med* 61:686–95

Girouard H, Iadecola C (2006) Neurovascular coupling in the normal brain and in hypertension, stroke, and Alzheimer disease. *J Appl Physiol* 100:328–35

Gonzalez-At JB, Alsop DC, Detre JA (2000) Cerebral perfusion and arterial transit time changes during task activation determined with continuous arterial spin labeling. *Magn Reson Med* 43:739–46

Grandin CB, Bol A, Smith AM, Michel C, Cosnard G (2005) Absolute CBF and CBV measurements by MRI bolus tracking before and after acetazolamide challenge: repeatabilily and comparison with PET in humans. *Neuroimage* 26:525–35

Gunther M, Oshio K, Feinberg DA (2005) Single-shot 3D imaging techniques improve arterial spin labeling perfusion measurements. *Magn Reson Med* 54:491–8

Herscovitch P, Raichle ME (1985) What is the correct value for the brain—blood partition coefficient for water? *J Cereb Blood Flow Metab* 5:65–9

Hund-Georgiadis M, Zysset S, Naganawa S, Norris DG, Von Cramon DY (2003) Determination of cerebrovascular

reactivity by means of FMRI signal changes in cerebral microangiopathy: a correlation with morphological abnormalities. *Cerebrovasc Dis* 16:158–65

Jenkinson M, Smith S (2001) A global optimisation method for robust affine registration of brain images. *Med Image Anal* 5:143–56

Johansen-Berg H (2007) Functional imaging of stroke recovery: what have we learnt and where do we go from here? *Int J Stroke* 2:7–16

Kim J, Whyte J, Patel S, Europa E, Slattery J, Coslett HB, Detre JA (2012) A perfusion fMRI study of the neural correlates of sustained-attention and working-memory deficits in chronic traumatic brain injury. *Neurorehabil Neural Repair*; advance online publication, 22 February 2012; doi:10.1177/1545968311434553

Langhorne P, Williams BO, Gilchrist W, Howie K (1993) Do stroke units save lives? *Lancet* 342:395–8

Leenders KL, Perani D, Lammertsma AA, Heather JD, Buckingham P, Healy MJ, Gibbs JM, Wise RJ, Hatazawa J, Herold S, Beaney RP, Brooks DJ, Spinks T, Rhodes C, Frackowiak RSJ, Jones T (1990) Cerebral blood flow, blood volume and oxygen utilization. Normal values and effect of age. *Brain* 113(Part 1):27–47

Lu H, Golay X, Pekar JJ, Van Zijl PC (2003) Functional magnetic resonance imaging based on changes in vascular space occupancy. *Magn Reson Med* 50:263–74

Lu H, Clingman C, Golay X, van Zijl PC (2004) Determining the longitudinal relaxation time (T1) of blood at 3.0 Tesla. *Magn Reson Med* 52:679–82

Lu H, Nagae-Poetscher LM, Golay X, Lin D, Pomper M, van Zijl PC (2005) Routine clinical brain MRI sequences for use at 3.0 Tesla. *J Magn Reson Imaging* 22:13–22

MacIntosh BJ, Filippini N, Chappell MA, Woolrich MW, Mackay CE, Jezzard P (2010*a*) Assessment of arterial arrival times derived from multiple inversion time pulsed arterial spin labeling MRI. *Magn Reson Med* 63:641–7

MacIntosh BJ, Lindsay AC, Kylintireas I, Kuker W, Gunther M, Robson MD, Kennedy J, Choudhury RP, Jezzard P (2010*b*) Multiple inflow pulsed arterial spin-labeling reveals delays in the arterial arrival time in minor stroke and transient ischemic attack. *AJNR Am J Neuroradiol* 31:1892–4

Mandell DM, Han JS, Poublanc J, Crawley AP, Stainsby JA, Fisher JA, Mikulis DJ (2008) Mapping cerebrovascular reactivity using blood oxygen level-dependent MRI in Patients with arterial steno-occlusive disease: comparison with arterial spin labeling MRI. *Stroke* 39: 2021–8

Mustanoja S, Meretoja A, Putaala J, Viitanen V, Curtze S, Atula S, Artto V, Happola O, Kaste M (2011) Outcome by stroke etiology in patients receiving thrombolytic treatment: descriptive subtype analysis. *Stroke* 42: 102–6

Newton J, Sunderland A, Butterworth SE, Peters AM, Peck KK, Gowland PA (2002) A pilot study of event-related functional magnetic resonance imaging of monitored wrist movements in patients with partial recovery. *Stroke* 33:2881–7

Ogawa S, Lee TM, Kay AR, Tank DW (1990) Brain magnetic resonance imaging with contrast dependent on blood oxygenation. *Proc Natl Acad Sci USA* 87:9868–72

Pineiro R, Pendlebury S, Johansen-Berg H, Matthews PM (2002) Altered hemodynamic responses in patients after subcortical stroke measured by functional MRI. *Stroke* 33:103–9

Poser BA, Norris DG (2011) Application of whole-brain CBV-weighted fMRI to a cognitive stimulation paradigm: robust activation detection in a stroop task experiment using 3D GRASE VASO. *Hum Brain Mapp* 32:974–81

Raichle ME, Mintun MA (2006) Brain work and brain imaging. *Annu Rev Neurosci* 29:449–76

Roc AC, Wang J, Ances BM, Liebeskind DS, Kasner SE, Detre JA (2006) Altered hemodynamics and regional cerebral blood flow in patients with hemodynamically significant stenoses. *Stroke* 37:382–7

Rossini PM, Altamura C, Ferretti A, Vernieri F, Zappasodi F, Caulo M, Pizzella V, Del Gratta C, Romani GL, Tecchio F (2004) Does cerebrovascular disease affect the coupling between neuronal activity and local haemodynamics? *Brain* 127:99–110

Williams DS, Detre JA, Leigh JS, Koretsky AP (1992) Magnetic resonance imaging of perfusion using spin inversion of arterial water. *Proc Natl Acad Sci USA* 89:212–6

Zhou J, van Zijl PC (1999) Effect of transit times on quantification of cerebral blood flow by the FAIR T(1)-difference approach. *Magn Reson Med* 42:890–4

Supplementary Information accompanies the paper on the Journal of Cerebral Blood Flow & Metabolism website (http://www.nature.com/jcbfm)